IEEE Access
Multidisciplinary ⋮ Rapid Review ⋮ Open Access Journal

Received 12 March 2026, accepted 31 March 2026, date of publication 6 April 2026, date of current version 14 April 2026.

Digital Object Identifier 10.1109/ACCESS.2026.3681387

RESEARCH ARTICLE

Micromobility Vehicle Classification for Smart City Infrastructure Using Magnetic Field Sensor Array

EIDENIS KASPERAVIČIUS[1], DANGIRUTIS NAVIKAS[1], VYTAUTAS MARKEVIČIUS[1], ALGIMANTAS VALINEVIČIUS[1], MINDAUGAS ŽILYS[1], MINDAUGAS ČEPĖNAS[1], JOŽEF RITONJA[2], (Member, IEEE), DARDAN KLIMENTA[3], NIKOLAY HINOV[4], AND DARIUS ANDRIUKAITIS[1], (Member, IEEE)

[1]Department of Electronics Engineering, Faculty of Electrical and Electronics Engineering, Kaunas University of Technology, 51368 Kaunas, Lithuania
[2]Faculty of Electrical Engineering and Computer Science, University of Maribor, 2000 Maribor, Slovenia
[3]Faculty of Technical Sciences, University of Priština in Kosovska Mitrovica, 38220 Kosovska Mitrovica, Serbia
[4]Faculty of Computer Systems and Technologies, Technical University of Sofia, 1000 Sofia, Bulgaria

Corresponding author: Darius Andriukaitis (darius.andriukaitis@ktu.lt)

This work was supported in part by the Research Council of Lithuania (LMTLT) and the Ministry of Education, Science and Sport of the Republic of Lithuania, under Agreement S-A-UEI-23-1.

ABSTRACT Urban mobility worldwide is seeing an increasing use of micromobility vehicles such as bicycles and e-scooters. However, accurate methods for measuring their traffic parameters remain limited, which could result in outdated infrastructure planning practices. Conventional sensing technologies such as pneumatic tubes, computer vision, and inductive loops struggle with the small dimensions, low metal content, and high maneuverability of micromobility vehicles. This work presents an experimental classification method based on magnetic signatures, which is designed for micromobility traffic monitoring in smart city applications. A sensor array consisting of 11 magnetic field sensors installed across a bicycle path was used to collect 236 real-world vehicle signatures. Fourteen temporal, spatial, and frequency-domain features were extracted from each signature and evaluated using multiple machine learning models. Gradient Boosting model achieved the highest performance with a cross-validation accuracy of 82%, demonstrating that magnetic field signatures contain sufficient information to differentiate bicycles, e-scooters, and heavy micromobility vehicles. Even with a limited dataset, results demonstrate the feasibility of micromobility traffic monitoring based on magnetic signatures. Expanding the dataset and implementing additional signal processing algorithms is expected to further enhance classification accuracy and support safe and accessible mobility in smart cities.

INDEX TERMS Micromobility, smart cities, traffic monitoring, magnetic sensors, machine learning.

I. INTRODUCTION

Urban mobility worldwide is undergoing a transformation directed towards addressing ecological challenges and improving the efficiency and accessibility of everyday travel. First- and last-mile travel as a transport mode gap has been recently addressed by micromobility vehicles – light (up to 350 kg), low-speed (up to 45 km/h) powered or unpowered vehicles often designed for single users [1]. Their adoption is growing fast: large European cities are building almost 1500 km of bicycle paths per year [2], while the number of shared micromobility trips in North America has increased by 20% from 2022 to 2023 [3]. However, urban infrastructure design still primarily targets bicycles, instead of accommodating for the wider range of powered micromobility vehicles such as e-scooters [2], resulting in potentially outdated planning practices.

Successful smart city planning requires accurate measurements of traffic parameters, including aggregate statistics (traffic density, predominant directions), individual vehicle

The associate editor coordinating the review of this manuscript and approving it for publication was Wenbing Zhao.

© 2026 The Authors. This work is licensed under a Creative Commons Attribution 4.0 License.
For more information, see https://creativecommons.org/licenses/by/4.0/

parameters (type, length, etc.) and user behavior parameters (speed, route choice, etc.) [4]. In this regard, the effect of micromobility vehicles is significant - research has shown that the increasing traffic flow of light vehicles (such as bicycles and mopeds) alters traffic flow dynamics of the entire city [5]. Real-time data of technical parameters such as traffic flow, composition of different vehicle types and driving speeds can be used for optimizing technical infrastructure [6], road capacity and safety [7] and other areas.

While such parameters are easily monitored for conventional traffic, there is a lack of methods applicable to micromobility vehicles (Table 1). Conventional sensors are often unsuitable due to small vehicle dimensions, high maneuverability, low clearance and low amount of metal parts [8]. For example, contact measurement methods such as pneumatic tubes or piezoelectric sensors are simple to use and inexpensive, however, the lower clearance of micromobility vehicles may impact measurement device selection, while reduced degree of physical protection of micromobility users can cause safety concerns [9]. Video based methods can offer high accuracy for traditional vehicles, e.g. 92% [10], but the accuracy for micromobility is often much lower – e.g. 44% for skateboards, 66% for scooters [11]. In addition, the accuracy of visual methods depends on the time of day, lighting and weather conditions [12]. Magnetic field sensors offer a promising alternative: they are cost-efficient, resistant to environmental factors, and are relatively simple to install. Methods using magnetic field sensors can also be easily adapted to accommodate small, maneuverable micromobility vehicles, as earlier studies have shown that vehicle movement induces measurable magnetic field disturbances [13].

In the context of magnetic field sensors, the type (class) of a vehicle is the most difficult parameter to measure of all listed previously, compared to linear parameters such as driving direction or speed. The task is further complicated by the ambiguity of definitions – multiple classification types are available. For example, SAE International excludes unpowered vehicles and classifies the rest by vehicle configuration [14], while the International Transport Forum report includes unpowered vehicles and classifies by speed and weight [15]. For specific applications, the defined classes can be adjusted based on the properties of the local micromobility traffic.

Building on existing classifications, this paper introduces a method for micromobility vehicle classification using magnetic field sensor arrays, which has not been explored previously. The approach aims to improve the accuracy and reliability of micromobility traffic parameter measurement, supporting the infrastructure planning, traffic management and urban mobility optimization in smart cities.

II. RELATED WORKS

In modern research, micromobility is increasingly framed as a critical system for transitioning towards the new generation of smart city models and creating the *digital urban commons* [16]. From a policy perspective, micromobility is a tool for smart urban growth, sustainably increasing density and providing essential first-and-last mile connectivity to public transit hubs [17], [18] by providing a price-efficient alternative to car ownership and supporting the Avoid-Shift-Improve triad (a shift from private motorized transport to more sustainable travel modes) [18], [19].

More specifically, the monitoring of micromobility traffic is essential in sustainable urban planning frameworks such as the CalmMobility paradigm, which advocates for a deliberate pace and sequencing of change over disruptive implementation [19]. Reliable micromobility detection and classification systems provide high-granularity data needed for ''go/adjust/stop'' gates in pilot projects that are evidence-based and reversible [19], [20]. Such systems allow for targeted implementation of road safety measures and ultimately result in calmer and safer urban environments [17], [19], [20].

A. MICRMOBILITY VEHICLE PARAMETER MEASUREMENT METHODS

Despite its importance for urban planning, research on micromobility traffic parameter measurement remains limited; the number of papers published within the last three years does not exceed ten [21]. Most existing research focuses computer vision approaches (most commonly YOLO models) with mixed results.

A 2021 study using 229 images of naturalistic scenes achieved an accuracy above 91% for binary classification (''e-scooter rider'' and ''non-rider'') but occlusions remained a significant limitation [22]; a 2024 study employing a substantially larger dataset demonstrated that accuracy for certain micromobility classes can be as low as 44% [11]. Another research direction involves active micromobility identification, where, in which micromobility riders are equipped with, for example, backscatter tags compatible with automotive radar systems [23]. However, such approaches require large-scale regulatory adoption before becoming universally applicable.

The feasibility of using magnetic field sensors to measure micromobility vehicle parameters does not depend on recent technological advancements. In 2014, the US Federal Highway Administration reported that a pair of magnetic field sensors separated by 0.9 m can detect a bicycle from 1.2 m distance [24]. However, there are no commercial or published experimental systems which would use this type of sensor.

Magnetic field sensors have been successfully used for conventional vehicle detection. For example, researchers have achieved a vehicle counting accuracy of 92-95% using such sensor type [25]. While a single sensor is not enough to detect driving direction or perform classification, methods using several sensors have achieved a speed estimation accuracy of 7.5 km/h for 90% of vehicles and a classification accuracy of 87% [26]. Even better accuracy has been achieved by using a time-synchronized sensor array. Such system is

TABLE 1. Summary of vehicle parameter measurement methods potentially usable for micromobility.

Method	Advantages	Limitations
Contact sensors (pneumatic/piezoelectric)	Simple, low cost, reliable	Safety concerns for micromobility vehicle riders; not optimized for low weight vehicles
Video-based methods	Non-intrusive deployment, rich data	Low accuracy for micromobility (e.g. 66%), susceptible to weather and lighting conditions, occlusions
Inductive loops	High SNR and classification accuracy (e.g. 95%); mature for conventional vehicles	Large footprint (complex deployment, susceptible to mechanical wear), low transverse resolution
Single magnetic field sensor	Small footprint, low cost, simple deployment	Cannot determine direction or vehicle class
Magnetic field sensor array	Capable of classification, high spatial resolution, smaller footprint than inductive loops	More difficult synchronization and signal processing

also capable of re-identification of vehicles (recognizing the same vehicle from a pool of candidates) with 90% accuracy [27]. Still, this technology has not yet been evaluated in a micromobility context.

Inductive loops, another method commonly used in conventional vehicle parameter measurement, have recently been adapted for micromobility. Researchers in Valencia [4] announced their work on a double 0.5 m loop working at 400-800 kHz frequency, which captures the micromobility vehicle's inductive profile, calculates the profile's parameters and estimates the vehicle's parameters. More recently, other researchers [8] described their own differently sized inductive loops (100 cm width, 22-92 cm length), which are measured at 1 MHz frequency and achieve significant signal-to-noise ratio. A commercial solution is available as well – the ZELT range by Eco-Counter includes bicycle counters which can distinguish two classes (bicycles and scooters) with accuracy of 95% using 13 differentiation criteria [28].

However, inductive loop measurements have significant disadvantages compared to magnetic field sensors. The size of the loop is relatively large, which results in a large area of the road surface excavated during installation. It also leads to significantly worse spatial resolution perpendicular to the driving direction. Moreover, the mechanical construction of the loop wears out over time due to road deterioration or heavy vehicles [29].

Magnetic field sensors offer advantages in smaller footprint and increased spatial resolution, which can improve the accuracy and reliability of the traffic parameter measurement devices. In addition, these sensors are easier to deploy and maintain – unlike inductive loops (which may need to have their sensitivity adjusted on changes in the environment, and a large road area maintained for mechanical damage) and unlike video-based methods (which need ROI selection and lens cleaning), magnetic field sensors offer automatic self-calibration, adapt to changes in the environment (temperature, nearby metallic or magnetic objects) and only require maintenance of a small strip of road surface.

B. MAGNETIC VEHICLE SIGNATURE PROCESSING

After capturing a vehicle's magnetic signature, processing is required to estimate vehicle parameters. One such method is rule-based classification - one of the most straightforward techniques. For example, direct rules were used to classify cars according to their signature lengths [25]. However, the accuracy was poor - less than 8% for some classes. A more effective approach combines multiple features – for example, one system used three features (normalized magnetic length, averaged energy and number of peaks in hill pattern) fed into a hierarchical tree with manually configured thresholds [30]. This resulted in an implementation suitable for a resource-constrained microprocessor, while achieving 80.9% accuracy. However, micromobility vehicles are smaller and more variable, thus more difficult to detect. For such signals, a small number of features is likely to result in poor performance, while a tree with many features is impractical to optimize manually.

Machine learning (ML) models are the modern solution for improving accuracy. To achieve stable and accurate results, features such as peak amplitudes, relative positions or signature length are extracted from magnetic signatures. The process of feature selection can either be done manually or automatically, using dimensionality reduction techniques [31].

Various ML models have been used for *conventional* vehicle classification. Since simple probabilistic models like Naïve Bayes and Logistic Regression perform poorly for nonlinear problems and correlated features [31], they are usually not used for magnetic signature processing. Decision trees have achieved over 80% accuracy in some signature classification studies [32], [33] but suffer from overfitting and poor performance with large datasets [31]. Support Vector Machines (SVM) have also shown good performance. For example, SVM models using just two magnetic-based features (amplitude ratio and signature length) reached 83% vehicle classification accuracy [34].

Ensemble methods such as Random Forests, Gradient Boosted Trees, and AdaBoost generally outperform individual models in classification tasks [31] - for example, AdaBoost model with an SVM core achieved up to 94.6% accuracy for conventional vehicle classification [35]. Comparative studies suggest that ensemble-based approaches provide the best trade-off between accuracy and robustness for magnetic-signature-based vehicle classification [35], [36], while deep neural networks require significant computational resources, large amounts of training data and long training times [31].

In summary, magnetic field sensors have been tested and proven effective for conventional vehicle detection and classification but remain unexplored for micromobility vehicles. Addressing this gap could lead to more accurate monitoring of micromobility traffic, better infrastructure planning for smart cities, and improved safety for users of these light, highly maneuverable vehicles.

III. METHODOLOGY

The main classification principle described in this paper is based on collecting magnetic signatures of micromobility vehicles driving along a bicycle path and passing over a temporarily installed measurement system. The overall structure of the system used for experiments is presented in Fig. 1. It consisted of:

1) *11 magnetic field sensors* spaced in 10 cm intervals across the bicycle path (spacing obtained from initial simulations).
2) *Sensor hub*, which sampled magnetic field sensors at 500 Hz, removed temperature-dependent offset drift, performed simple threshold-based vehicle detection (signature start and end detection) and stored captured signatures in memory.
3) *Computer*, which connected to the hub, downloaded collected signatures for asynchronous processing and captured camera footage for evaluation. Time synchronization was achieved using a public NTP server.

Examples of captured micromobility vehicle signatures are shown in Fig. 2.

Based on the local vehicle type distribution in local traffic, the micromobility vehicle classes used in this paper (Table 2) were adapted from SAE International [14]. The bicycle and e-scooter classes were kept, while the heavy micromobility class was created to group less common vehicles - powered bicycles (e-bikes) and seated scooters.

The typical signatures of different vehicle classes (Fig. 2) have distinctive features. For example, the bicycle signature has two narrow peaks (wheels), the e-scooter signature includes the internal battery (between the wheels) and the heavy micromobility signature has a relatively large spatial width.

Captured signatures were processed using the pipeline outlined in Fig. 3. First, the stored data was cleaned to remove

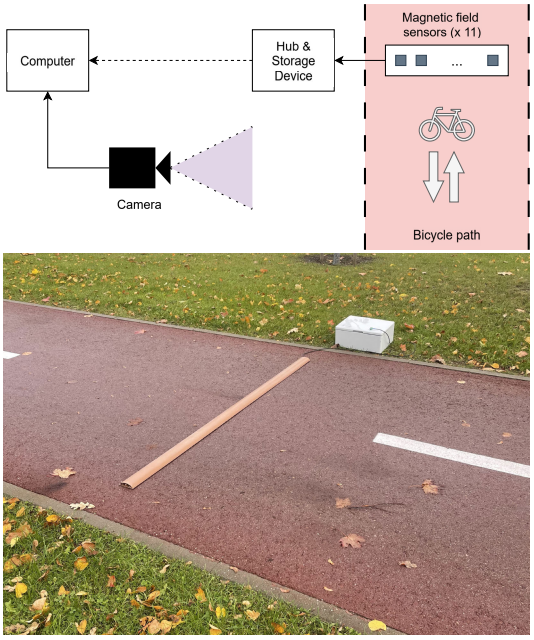

FIGURE 1. Data collection system.

TABLE 2. Adapted micromobility vehicle classification.

Class	Description	Included vehicles
Bicycles	Unpowered light (<35 kg) vehicles	Bicycles
E-scooters	Powered light (<35 kg) slow (<25 km/h) vehicles	Rental and personal standing e-scooters
Heavy micromobility	Powered heavy (>35 kg) or fast (>25 km/h) vehicles.	Light and heavy e-bikes; rental and personal e-scooters

incorrectly recorded signatures. Afterwards, signatures were manually labelled using recorded camera footage.

A time-domain signal was extracted from each signature for feature calculation. Since the measurement system can be oriented in any compass direction and the Earth's magnetic field has a horizontal component (the magnetic inclination is not 90° except for the poles), the x and y axis data of the captured signatures depend on the sensor orientation. To reduce the system's sensitivity to orientation, the z axis of the magnetic field B_z was selected instead of the magnitude.

To prepare for signature classification, the center sensor of each signature with index c was selected according to

$$c = \arg\max_j \left(\max_i \left(|z_{i,j}| \right) \right), \tag{1}$$

where $z_{i,j}$ is the magnetic field value at time i and sensor index j, resulting in the sensor which has the largest absolute

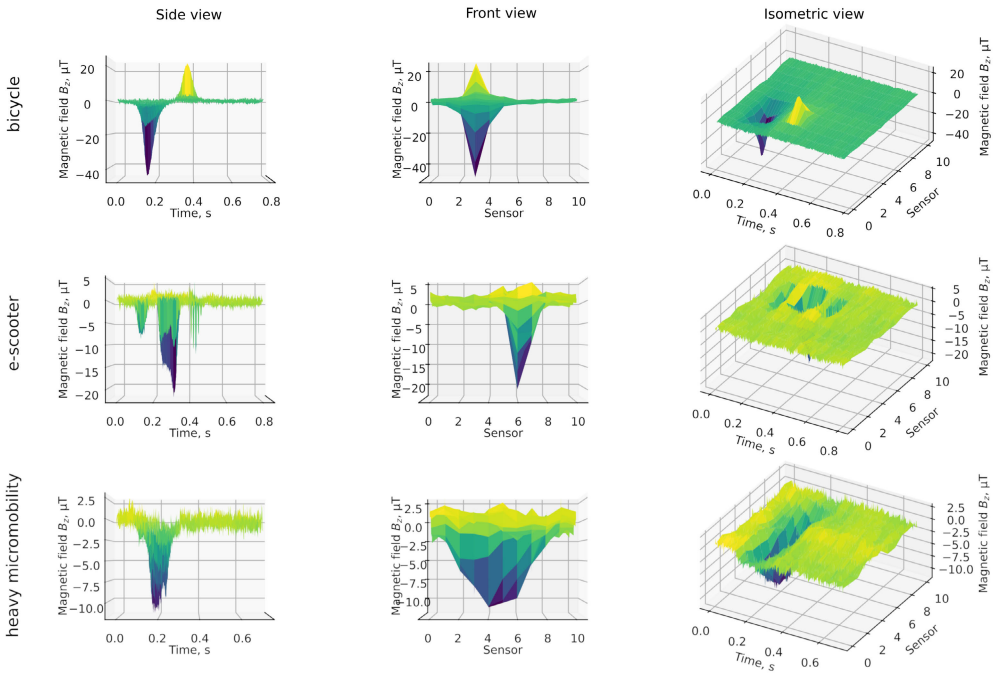

FIGURE 2. Typical magnetic signatures of micromobility vehicles.

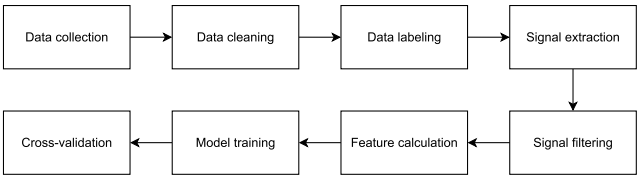

FIGURE 3. Data processing pipeline.

maximum of its time series data. It is visible in the middle column of Fig. 2.

Each selected signal was filtered with a low-pass filter before performing feature extraction. The filter parameters (cutoff frequency $f_c = 30$ Hz) were selected experimentally, based on the spectral contents of collected vehicle signatures.

The features used for machine learning (Fig. 4) were selected iteratively. Starting from a list of 35 features, the feature with the lowest cross-validation importance was recursively eliminated. The process was repeated to remove the maximum number of features until the accuracy started to drop. The best performing features were extracted from the signal B_z of the center sensor (except for spatial features).

The feature set included both features from existing research and original features (Table 3).

The temporal, spatial and frequency features were selected to capture the main noticeable differences between signatures of different vehicle classes, while more complex features (ratios) were designed to aid in classifying atypical signatures.

Lastly, the extracted feature vectors were passed to selected machine learning models (Gradient Boosting, Random Forest, support vector machine, k-Nearest Neighbors (KNN), Naïve Bayes and Logistic Regression) for training and validation. Stratified 10-fold cross-validation was used to reduce the evaluation bias and obtain accurate results.

IV. RESULTS

236 valid micromobility vehicle signatures were collected under real traffic conditions (Table 4). The overall traffic density (including valid and discarded samples), measured in 15-minute intervals, ranged from 20 to 76 vehicles per hour, with an average of 31.3 vehicles per hour. Most discarded signatures resulted from vehicles not passing correctly over the temporarily installed measurement system. A smaller number of signatures (predominantly bicycles) were discarded due to micromobility users travelling in groups and crossing the measurement device in short succession, resulting in a multi-vehicle signature.

Most of the valid data (59.7%) consists of bicycle signatures, 26.3% - e-scooters, 14% - heavy micromobility signatures. Other discarded signatures include mobility scooters, lawn mowers, etc. This dataset represents real-world conditions, as it was collected from actual campus micromobility traffic rather than simulated or artificial traffic.

Using the features described previously, machine learning models were trained and evaluated using cross-validation. The mean accuracy for all models (Table 5) was similar (0.7 to 0.82), but the standard deviation varied up to 2.5 times (0.04 to 0.11). Simple models based on assumptions about the data (Logistic Regression, Naïve Bayes) performed worse

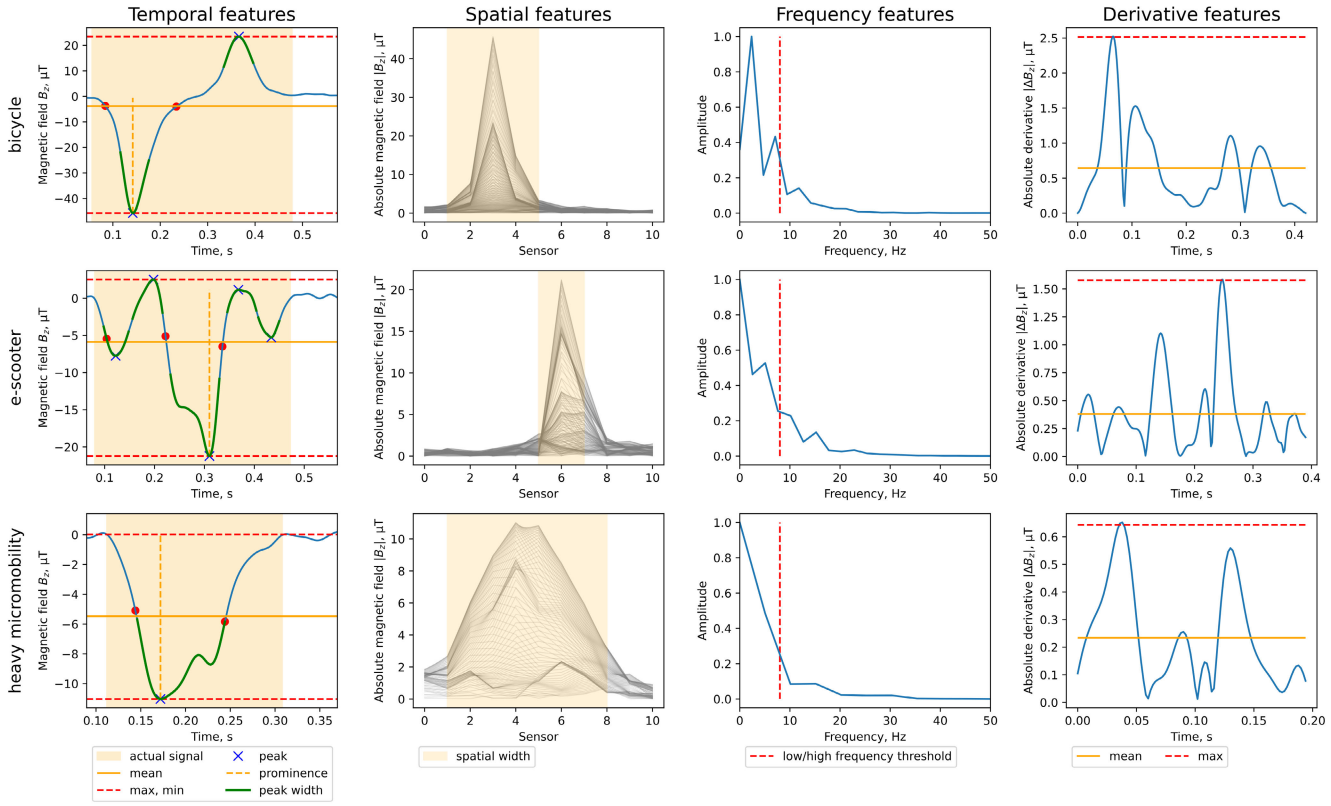

FIGURE 4. Examples of features extracted from vehicle magnetic signatures.

than more complex models due to the classification problem being complex (nonlinear) itself.

For all models, the accuracy was higher than the random uniform prediction baseline of 0.33 and majority class (bicycle) prediction baseline of 0.60 (with p-values significantly below $\alpha = 0.05$), which proves the value of application of the evaluated models.

The best cross-validation accuracy of 0.82 ± 0.04 was achieved with the Gradient Boosting model. The result is sufficient for an experimental model with a limited dataset. The best-recognized class (Fig. 5) was bicycles with recall of 0.89 and precision of 0.83, followed by e-scooters with recall of 0.76 and precision of 0.83. The main issues were related to the low number of heavy micromobility samples – the model reached a recall of only 0.64 and precision of 0.75. The macro-average F1 score is 0.78 (with each class given an equal weight).

The other two best-performing models (Random Forest and SVM) achieved similar results, but the per-class metrics varied. According to McNemar's tests comparing all models against the Gradient boosting model, Random Forest is the only model with no significant statistical difference in classification results (all other p-values significantly below $\alpha = 0.05$). The Random Forest model performed worse in classifying heavy micromobility, lowering recall to 0.45. SVM improved heavy micromobility classification to an accuracy of 0.73 at the cost of reducing other class accuracies to a similar level.

The results of the best performing model (Gradient Boosting) were analyzed in more detail. One important observation was that dataset augmentation (increasing the amount of heavy micromobility samples through signal inversion) achieved marginal improvement (accuracy of 0.84) but increased standard deviation by almost 40% (to 0.06). Since only two of the used features are asymmetric, signal inversion did not substantially increase the variability of the heavy micromobility class. As a result, the model improved its performance on samples similar to those already observed, while becoming more sensitive to fold-specific variations in the training data.

Other imbalance handling techniques such as class weight adjustment or majority class undersampling achieved results similar to those of the SVM. Increasing the weight of the heavy micromobility class improved its accuracy (up to a maximum of 0.77) but reduced the overall accuracy and increased standard deviation across folds for the same reason observed with the inversion augmentation.

On the other hand, increasing the number of real heavy micromobility samples should improve model accuracy because the learning curve (Fig. 6) did not reach its plateau for validation data.

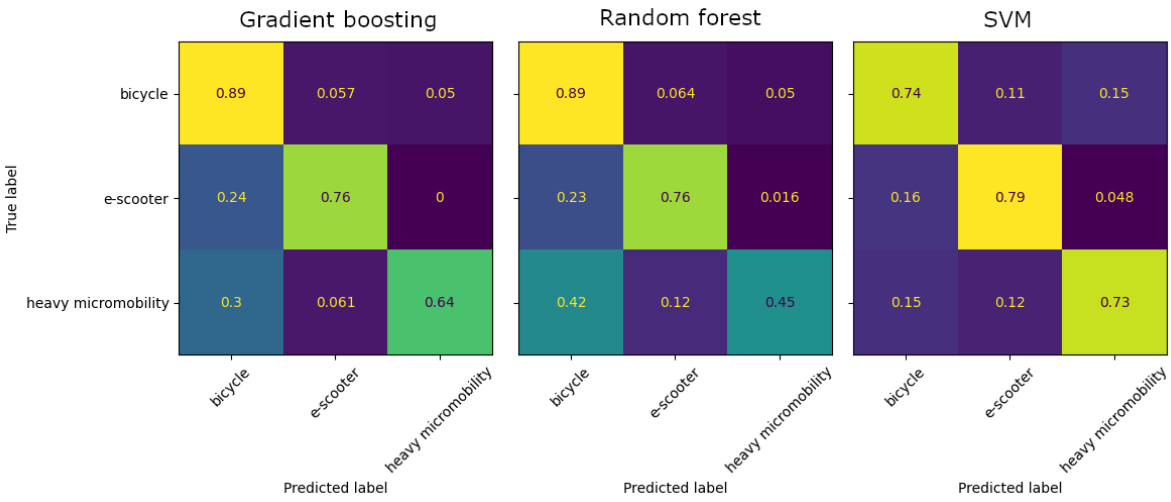

FIGURE 5. 10-fold cross-validation confusion matrix of the three best performing classifiers, normalized to number of true samples.

It is important to note that the training accuracy curve reached saturation when 25% of the training data was used. This indicates overfitting, which arises because the Gradient boosting model quickly memorizes patterns in the limited set (N=236). However, the cross-validation accuracy, evaluated on signatures not seen during training, is relatively high and continues to increase, showing that the model can classify unseen vehicles. The overfitting primarily reflects the small dataset rather than a fundamental flaw in the model, since experiments with simpler models did not result in improved performance. Adding more samples, particularly for the heavy micromobility class, would improve generalization.

Based on the underlying data of the learning curve, it was estimated that the heavy micromobility class recall would plateau at 0.7 with at least 1000 total samples (keeping the existing class proportions), while the overall accuracy would plateau at 0.88 with 500 total samples. This is confirmed by existing research – Gradient Boosting models need at least 20-30 samples per feature, depending on the complexity of the data [38]. Moreover, it is likely that additional heavy micromobility signatures would allow for the extraction of more informative features, which would improve the accuracy further. The accuracy needed for practical deployments varies, but is usually 90% to 95% in commercial systems [28].

The feature list described previously was selected from a broader feature list by evaluating the accuracy curve (Fig. 7). The maximum accuracy point before the plateau is 14 - increasing the number of features further did not improve the accuracy but reduced model stability.

Of all the used features, two were significantly more important than others (Fig. 8): low/high frequency energy ratio at 19% (suggesting that heavy micromobility signatures are likely to have fewer high frequency components than

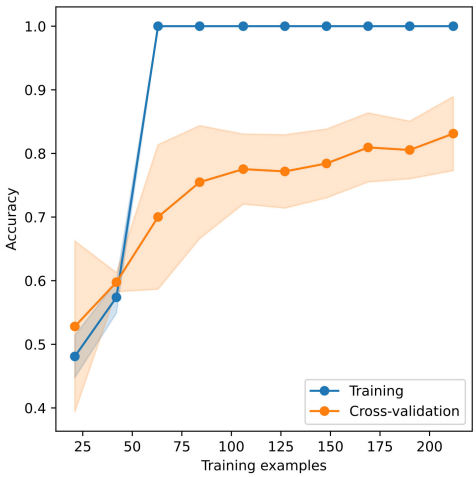

FIGURE 6. Gradient Boosting model cross-validation learning curve, shaded area – standard deviation.

bicycles or e-scooters) and spatial width at 12% (suggesting that magnetic field disturbances caused by heavy micromobility have a greater area of effect than those of smaller, lighter vehicles). The rest of the feature importances gradually drop off to just above 3.5%.

In summary, the results demonstrate that magnetic signature features, used as inputs for a Gradient Boosting model, are sufficient for micromobility vehicle classification. However, a larger and more balanced dataset is needed to reach performance sufficient for urban planning applications.

V. LIMITATIONS

While the proposed micromobility classification method avoids many drawbacks of alternative sensing technologies (e.g., it is not sensitive to pedestrians or micromobility vehicle

TABLE 3. Used features.

	Feature name	Comment
1	Number of peaks [8], [36]	Number of local extrema
2	Average peak-to-peak distance [8]	Average distance between local extrema
3	Peak width [36]	Average local extrema width
4	Prominence [8]	Average local extrema prominence
5	Effective signal length	The length of the widest interval where any sample of the signal is above 2.3 µT (threshold selected as 50% over the measured noise amplitude of 1.5 µT), extended outwards to the nearest zero sample
6	Full peak width	The length of the interval from the peak to the nearest zero samples in both directions
7	Standard deviation of the effective signal [36], [37]	Standard deviation of the effective signal
8	Position of global minimum [37]	Normalized as $p_{min} = \frac{arg\,min(z)}{l_e}$, where l_e is effective signal length, *arg min (z)* is the index of the minimum sample
9	Position of first local minimum [37]	
10	Position of first mean crossing [37]	
11	Spatial width $w_{spatial}$	The length of the interval (number of sensors) where the sample at time i of maximum sample $z_{i,j}$ is above 2.3 µT (same threshold as previously)
12	Low/High frequency energy ratio	Spectrum-based ratio $R_E = \frac{\sum_{f=0}^{f_{th}} \lvert Z[f]\rvert^2}{\sum_{f=f_{th}}^{f_s/2} \lvert Z[f]\rvert^2}$, where Z[f] is spectral amplitude at frequency f, f_{th}=8 Hz is the iteratively selected threshold between low and high frequencies, and f_s=500 Hz is the sample rate
13	Weight ratio R_w	Composite feature $R_w = w_{spatial} \cdot l_e \cdot \lvert z_{max}\rvert$.
14	Amplitude-variation ratio R_{av}	Composite feature $R_{av} = \frac{z_{max} - z_{min}}{\frac{1}{N-1}\sum_{n=0}^{N-2} \lvert z[n+1] - z[n]\rvert}$.

TABLE 4. Collected data.

	Discarded (in multi-vehicle signatures)	Discarded (vehicles not passing over the system)	Valid	Total
Bicycle	64	192	141	397
E-scooter	5	43	62	110
Heavy micromobility	-	7	33	40
Other	-	7	-	7

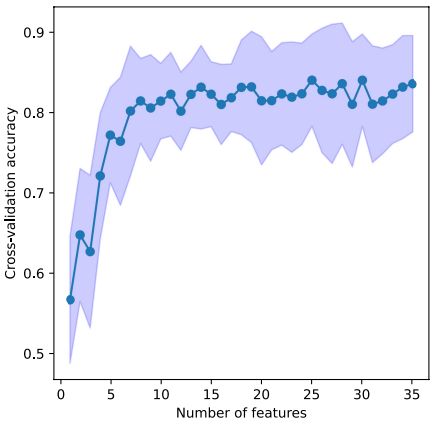

FIGURE 7. 10-fold cross-validation accuracy dependence on the number of features used, shaded area – standard deviation.

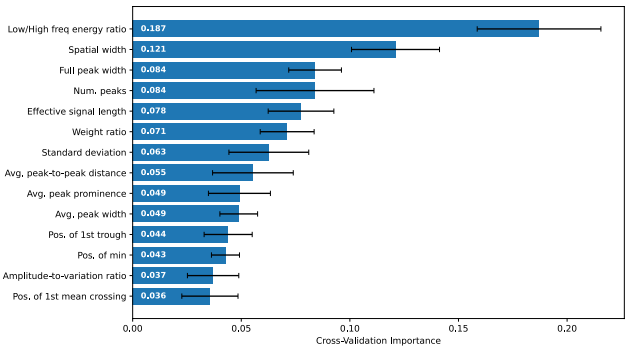

FIGURE 8. Gradient Boosting model feature importances and their standard deviations.

tire composition), it has its own limitations. In addition to the experimental constraints already discussed, such as the small dataset, the system cannot detect micromobility vehicles lacking metal or magnetic components. This includes devices such as kids scooters or rollerblades, which are generally not a significant part of micromobility traffic (less than 1% of all micromobility observed in this study). Moreover, the system's performance in extremely dense traffic, where riders maintain less than 10 cm of separation, remains uncertain, and it is unclear whether individual signatures could still be distinguished. Finally, the method cannot account for anomalous behaviours, such as riding a bicycle on one wheel.

TABLE 5. 10-fold cross-validation comparison of ML models (N=236).

Model	Accuracy ± std	Accuracy CI (95%)	Macro precision	Macro recall	Macro f1	t-test p-value*	McNemar's p-value**
Gradient Boosting	0.82 ± 0.04	0.80-0.84	0.80	0.76	0.78	$3.1 \cdot 10^{-8}$	-
Random Forest	0.79 ± 0.07	0.75-0.83	0.75	0.70	0.72	$1.3 \cdot 10^{-5}$	0.19
SVM (RBF kernel)	0.78 ± 0.08	0.73-0.83	0.70	0.75	0.71	$5.6 \cdot 10^{-5}$	0.02
KNN (k=5)	0.76 ± 0.05	0.73-0.79	0.71	0.67	0.69	$3.2 \cdot 10^{-6}$	0.04
Naïve Bayes	0.71 ± 0.07	0.67-0.75	0.63	0.65	0.64	$8.0 \cdot 10^{-4}$	$5.4 \cdot 10^{-4}$
Logistic Regression	0.70 ± 0.11	0.63-0.77	0.66	0.73	0.68	0.018	$1.8 \cdot 10^{-4}$
Majority class prediction baseline	0.60	-	-	-	-	-	-

* p-values from t-tests comparing each model against the majority class prediction baseline.

** p-values from McNemar's test comparing against Gradient Boosting model results.

VI. CONCLUSION

- The study demonstrated a proof of concept for micromobility vehicle classification using an array of 11 magnetic field sensors installed across a bicycle path. A total of 236 magnetic vehicle signatures were captured under real traffic conditions and classified into three classes (bicycles, e-scooters and heavy micromobility vehicles).
- A set of 14 features (temporal, spatial, frequency domain and others), combined with a Gradient Boosting model, resulted in the highest cross-validation accuracy of 82%. The most important features were the low/high frequency energy ratio and spatial width.
- This level of performance indicates that magnetic field sensor arrays have the potential to improve micromobility traffic parameter measurement compared with video-based methods (which report scooter detection accuracy as low as 66% due to sensitivity to weather and lighting, compared to 76% achieved in this study) and inductive loops (which achieve higher accuracy but only distinguish two classes and require more complicated deployment and maintenance).
- The main limitation of this study is the size and balance of the dataset, particularly the small number of heavy micromobility vehicle samples. Expanding the dataset to include a greater variety of vehicles is expected to improve classification performance and model generalization.

FUTURE WORK

Future work will focus on collecting a larger, more diverse dataset to improve model generalizability and address two key challenges observed during testing: (1) separation of overlapping vehicle magnetic signatures using neural networks for vehicle count estimation and signature segmentation or mix source separation techniques, and (2) re-alignment of signatures produced by vehicles crossing the sensor array diagonally using a vehicle axis estimation and rotation correction algorithm, or sensor fusion methods with gating mechanisms. Finally, before a measurement system based on this method is ready for deployment, its installation and maintenance procedures, scalability, and integration into smart city infrastructure must be addressed.

REFERENCES

[1] R. L. Abduljabbar, S. Liyanage, and H. Dia, "The role of micromobility in shaping sustainable cities: A systematic literature review," *Transp. Res. D, Transp. Environ.*, vol. 92, Mar. 2021, Art. no. 102734, doi: 10.1016/j.trd.2021.102734.

[2] M. Hossein Sabbaghian, D. Llopis-Castelló, and A. García, "A safe infrastructure for micromobility: The current state of knowledge," *Sustainability*, vol. 15, no. 13, p. 10140, Jun. 2023, doi: 10.3390/su151310140.

[3] NACTO. (2024). *Shared Micromobility Report: 2023*. Accessed: Oct. 07, 2025. [Online]. Available: https://nacto.org/publication/shared-micromobility-report-2023/

[4] M. Millana. *Personal Mobility Vehicle Monitoring System*. Accessed: May 15, 2025. [Online]. Available: https://www.itaca.upv.es/innovation-old/results-and-technology-offer/personal-mobility-vehicle-monitoring-system/

[5] R. Burdzik, I. Celinski, M. Ragulskis, V. Ranjan, and J. Matijosius, "Estimation of vehicle traffic parameters using an optical distance sensor for use in smart city road infrastructure," *J. Sensor Actuator Netw.*, vol. 13, no. 4, p. 35, Jun. 2024, doi: 10.3390/jsan13040035.

[6] Z. Dai, H. Song, H. Liang, F. Wu, X. Wang, J. Jia, and Y. Fang, "Traffic parameter estimation and control system based on machine vision," *J. Ambient Intell. Humanized Comput.*, vol. 14, no. 11, pp. 15287–15299, Nov. 2023, doi: 10.1007/s12652-020-02052-5.

[7] M. Kozerska, "Management of infrastructure and traffic volume versus road traffic safety," *Eur. Res. Stud. J.*, vol. 24, no. 3, pp. 615–632, Sep. 2021.

[8] T. P. Rajan and B. George, "An inductive loop detector for personal transporters in urban cycle lanes," in *Proc. 50th Annu. Conf. IEEE Ind. Electron. Soc.*, Nov. 2024, pp. 1–6, doi: 10.1109/IECON55916.2024.10905280.

[9] B. Stahl, J. Apfelbeck, and R. Lange, "Classification of micromobility vehicles in thermal-infrared images based on combined image and contour features using neuromorphic processing," *Appl. Sci.*, vol. 13, no. 6, p. 3795, Mar. 2023, doi: 10.3390/app13063795.

[10] D. Chen, A. Hosseini, A. Smith, A. Farzin Nikkhah, A. Heydarian, O. Shoghli, and B. Campbell, "Performance evaluation of real-time object detection for electric scooters," 2024, *arXiv:2405.03039*.

[11] K. Sabri, C. Djilali, G.-A. Bilodeau, N. Saunier, and W. Bouachir, "Detection of micromobility vehicles in urban traffic videos," 2024, *arXiv:2402.18503*.

[12] C.-Y. Chiang, M. Jaber, K. K. Chai, and J. Loo, "Distributed acoustic sensor systems for vehicle detection and classification," *IEEE Access*, vol. 11, pp. 31293–31303, 2023, doi: 10.1109/ACCESS.2023.3260780.

[13] V. Markevicius, D. Navikas, A. Daubaras, M. Cepenas, M. Zilys, and D. Andriukaitis, "Vehicle influence on the Earth's magnetic field changes," *Electron. Electr. Eng.*, vol. 20, no. 4, pp. 43–48, Apr. 2014, doi: 10.5755/j01.eee.20.4.4552.

[14] *Taxonomy and Classification of Powered Micromobility Vehicles*, document J3194_202502, SAE International Recommended Practice, Feb. 2025, doi: 10.4271/J3194_202502.

[15] A. Santacreu, G. Yannis, O. de S. Leon, and P. Crist. *Safe Micromobility*. Accessed: Oct. 7, 2025. [Online]. Available: https://www.itf-oecd.org/safe-micromobility

[16] F. Creutzig, "From smart city to digital urban commons: Institutional considerations for governing shared mobility data," *Environ. Research: Infrastructure Sustainability*, vol. 1, no. 2, Jul. 2021, Art. no. 025004, doi: 10.1088/2634-4505/ac0a4e.

[17] B. Fong, A. C. M. Fong, and G. Y. Hong, "Sustainable micromobility management in smart cities," *IEEE Trans. Intell. Transp. Syst.*, vol. 24, no. 12, pp. 15890–15896, Dec. 2023, doi: 10.1109/TITS.2023.3292377.

[18] J. C. Dias, P. Ribeiro, and E. Arsenio. (Sep. 2021). *Micromobility: A Systematic Literature Review on the Measurement of Its Environmental, Social, and Economic Impacts on Urban Sustainability*. [Online]. Available: https://hdl.handle.net/1822/78533

[19] K. Turon, "Sustainable urban mobility transitions—From policy uncertainty to the CalmMobility paradigm," *Smart Cities*, vol. 8, no. 5, p. 164, Oct. 2025, doi: 10.3390/smartcities8050164.

[20] P. Folco, L. Gauvin, M. Tizzoni, and M. Szell, "Data-driven micromobility network planning for demand and safety," *Environ. Planning B: Urban Analytics City Sci.*, vol. 50, no. 8, pp. 2087–2102, Oct. 2023, doi: 10.1177/23998083221135611.

[21] M. Hassanin, M. Abu Alsheikh, C. C. N. Kuhn, D. Herath, D. Thai Hoang, and I. Radwan, "Towards autonomous riding: A review of perception, planning, and control in intelligent two-wheelers," 2025, *arXiv:2507.11852*.

[22] K. Apurv, R. Tian, and R. Sherony, "Detection of E-scooter riders in naturalistic scenes," 2021, *arXiv:2111.14060*.

[23] A. Lazaro, M. Lazaro, R. Villarino, and D. Girbau, "Smart spread spectrum modulated tags for detection of vulnerable road users with automotive radar," *Sensors*, vol. 23, no. 5, p. 2730, Mar. 2023, doi: 10.3390/s23052730.

[24] Federal Highway Administration. *Office of Highway Policy Information - Policy | Federal Highway Administration*. Accessed: May 15, 2025. [Online]. Available: https://www.fhwa.dot.gov/policyinformation/pubs/vdstits2007/04pt2.cfm

[25] K. Culík, V. Štefancová, and K. Hrudkay, "Application of wireless magnetic sensors in the urban environment and their accuracy verification," *Sensors*, vol. 23, no. 12, p. 5740, Jun. 2023, doi: 10.3390/s23125740.

[26] Y. Feng, G. Mao, B. Chen, C. Li, Y. Hui, Z. Xu, and J. Chen, "MagMonitor: Vehicle speed estimation and vehicle classification through a magnetic sensor," *IEEE Trans. Intell. Transp. Syst.*, vol. 23, no. 2, pp. 1311–1322, Feb. 2022, doi: 10.1109/TITS.2020.3024652.

[27] J. Balamutas, D. Navikas, V. Markevicius, M. Cepenas, A. Valinevicius, M. Žilys, M. Prauzek, J. Konecny, Z. Li, and D. Andriukaitis, "Vehicle re-identification based on multiple magnetic signatures features evaluation," *IEEE Access*, vol. 12, pp. 102606–102618, 2024, doi: 10.1109/ACCESS.2024.3433615.

[28] *ZELT Evo—The World's Most Trusted Bike Counter | Eco-Counter*. Accessed: Oct. 13, 2025. [Online]. Available: https://www.eco-counter.com/solutions/counting-solutions/urban-zelt

[29] P. Beyer. *Non-Intrusive Detection, the Way Forward*. Accessed: Oct. 14, 2025. [Online]. Available: http://hdl.handle.net/2263/57785

[30] S. Keawkamnerd, J. Chinrungrueng, and C. Jaruchart, "Vehicle classification with low computation magnetic sensor," in *Proc. 8th Int. Conf. ITS Telecommun.*, Oct. 2008, pp. 164–169, doi: 10.1109/itst.2008.4740249.

[31] A. F. A. H. Alnuaimi and T. H. K. Al-Baldawi, "An overview of machine learning classification techniques," in *Proc. BIO Web Conf.*, vol. 97, 2024, p. 00133, doi: 10.1051/bioconf/20249700133.

[32] S. Kaewkamnerd, J. Chinrungrueng, R. Pongthornseri, and S. Dumnin, "Vehicle classification based on magnetic sensor signal," in *Proc. IEEE Int. Conf. Inf. Autom.*, Jun. 2010, pp. 935–939, doi: 10.1109/ICINFA.2010.5512140.

[33] J. Balamutas, M. Ambraziunas, D. Navikas, V. Markevicius, M. Cepenas, A. Valinevicius, M. Žilys, and D. Andriukaitis, "Method for accelerometer and magnetometer based vehicle classification," in *Proc. IEEE 26th Int. Conf. Intell. Transp. Syst. (ITSC)*, Sep. 2023, pp. 2289–2294, doi: 10.1109/ITSC57777.2023.10422711.

[34] S. Taghvaeeyan and R. Rajamani, "Portable roadside sensors for vehicle counting, classification, and speed measurement," *IEEE Trans. Intell. Transp. Syst.*, vol. 15, no. 1, pp. 73–83, Feb. 2014, doi: 10.1109/TITS.2013.2273876.

[35] H. Zhang, W. Zhou, G. Liu, Z. Wang, and Z. Qian, "Fine-grained vehicle make and model recognition framework based on magnetic fingerprint," *IEEE Trans. Intell. Transp. Syst.*, vol. 25, no. 8, pp. 8460–8472, Aug. 2024, doi: 10.1109/TITS.2024.3374888.

[36] H. Li, H. Dong, L. Jia, and M. Ren, "Vehicle classification with single multi-functional magnetic sensor and optimal MNS-based CART," *Measurement*, vol. 55, pp. 142–152, Sep. 2014, doi: 10.1016/j.measurement.2014.04.028.

[37] H. Dong, X. Wang, C. Zhang, R. He, L. Jia, and Y. Qin, "Improved robust vehicle detection and identification based on single magnetic sensor," *IEEE Access*, vol. 6, pp. 5247–5255, 2018, doi: 10.1109/ACCESS.2018.2791446.

[38] N. MacNell, L. Feinstein, J. Wilkerson, P. M. Salo, S. A. Molsberry, M. B. Fessler, P. S. Thorne, A. A. Motsinger-Reif, and D. C. Zeldin, "Implementing machine learning methods with complex survey data: Lessons learned on the impacts of accounting sampling weights in gradient boosting," *PLoS ONE*, vol. 18, no. 1, Jan. 2023, Art. no. e0280387, doi: 10.1371/journal.pone.0280387.

EIDENIS KASPERAVIČIUS received the bachelor's degree in electronics engineering from Kaunas University of Technology, in 2024, where he is currently pursuing the master's degree. He is with the Department of Electronics Engineering, Faculty of Electrical and Electronics Engineering, Kaunas University of Technology. His research interests include smart low-power sensors, intelligent transport systems, and the design of microprocessor systems.

DANGIRUTIS NAVIKAS received the M.Sc. degree in 1994 and the Ph.D. degree in electronics engineering in 1999. He is currently with the Department of Electronics Engineering, Faculty of Electrical and Electronics Engineering, Kaunas University of Technology. His research focuses on finding solutions for the issues related to the interactive design of microprocessor systems, integrated information systems, and WSN.

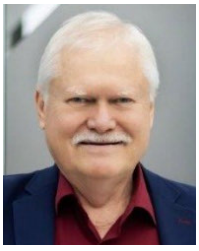

VYTAUTAS MARKEVIČIUS received the M.Sc. degree in 1973 and the Ph.D. degree in electronics engineering in 1983. He is currently with the Department of Electronics Engineering, Faculty of Electrical and Electronics Engineering, Kaunas University of Technology. He is the Leader of the research group on Interactive electronic systems. His research focuses on finding solutions for the issues related to interactive electronic systems, integrated information systems, energy harvesting, low power management, and WSN.

ALGIMANTAS VALINEVIČIUS received the M.Sc. degree in 1979 and the Ph.D. degree in electronics engineering in 1986. He is currently with the Department of Electronics Engineering, Faculty of Electrical and Electronics Engineering, Kaunas University of Technology. His research focuses on finding solutions for the issues related to interactive electronic systems, integrated information systems, and WSN.

MINDAUGAS ŽILYS received the M.Sc. degree in 1996 and the Ph.D. degree in electronics engineering in 2001. He is currently a Researcher with the Department of Electronics Engineering, Faculty of Electrical and Electronics Engineering, Kaunas University of Technology and in industry. His research focuses on electronic system efficiency, energy harvesting, low power management, and wireless smart sensors.

MINDAUGAS ČEPĖNAS received the master's degree in electronics engineering from Kaunas University of Technology (KTU), in 2012, and the Ph.D. degree in electronics engineering in 2018. He is currently a Researcher with the Department of Electronics Engineering, Kaunas University of Technology. His research interests include electronic system efficiency, energy harvesting, low power management, and wireless smart sensors.

JOŽEF RITONJA (Member, IEEE) received the B.S., M.S., and Ph.D. degrees in electrical engineering from the Faculty of Electrical Engineering and Computer Science, University of Maribor, in 1986, 1989, and 1996, respectively. Since 1987, he has been with the field of control theory and control applications with the Faculty of Electrical Engineering and Computer Science, University of Maribor, where he is currently a Professor and the Head of the Laboratory for Control and Electrical Machines.

DARDAN KLIMENTA was born in Serbia, in 1975. He received the degree from the Faculty of Electrical Engineering, University of Priština, in 1998, and the M.Sc. and Ph.D. degrees from the Faculty of Electrical Engineering, University of Belgrade, in 2001 and 2007, respectively. His main research interests include electrical power cable engineering, renewable energy sources, electric power system components, heat transfer, optimization methods, FEM, and FEA. He is currently a Full Professor with the Faculty of Technical Sciences, University of Priština in Kosovska Mitrovica.

NIKOLAY HINOV received the Ph.D. and D.Sc. degrees from the Technical University of Sofia, in 1998 and 2024, respectively. He is currently an Associate Professor with the Department of Computer Systems, Technical University of Sofia, Bulgaria. His research interests include artificial intelligence systems, development and design of power electronic converters with application in industrial technologies, electric vehicles, decentralized generation of electricity, and energy storage.

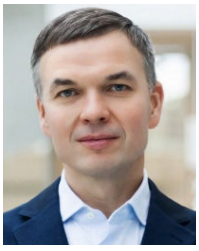

DARIUS ANDRIUKAITIS (Member, IEEE) received the M.Sc. degree in 2005 and the Ph.D. degree in electronics engineering in 2009. He is currently with the Department of Electronics Engineering, Faculty of Electrical and Electronics Engineering, Kaunas University of Technology. His research interests include interactive electronic systems, integrated information systems, smart transportation systems, control systems, the IoT and WSN.